Sciences with SuMIRe PFS Survey

Masahiro Takada (IPMU) and John D. Silverman (IPMU)

Executive Summary

The Subaru Measurement of Images and Redshifts (SuMIRe) is a joint experiment project of wide-field imaging and redshift surveys aimed at exploring the nature of dark energy as well as the growth of structure formation on cosmological scales by combining the *different* methods; weak gravitational lensing, baryonic acoustic oscillation (BAO), cluster counting statistics and probably also Type-Ia supernovae. By fully utilizing the unique capabilities of new prime-focus instruments, Hyper Suprime-Cam (HSC) and Prime-Focus Spectrograph (PFS), with about 1.5 degree diameter field-of-view, we can obtain imaging data of a billion of galaxies and redshifts of a few millions of galaxies (and QSOs). The requirements on the PFS design to maximize scientific outputs from the SuMIRe surveys are: 2000–3000 fibers to target 2200 galaxies per the PFS field-of-view and the spectral resolution $R \simeq 3000$ for wavelength coverage 600–1000nm in order to survey galaxies over redshift range $0.6 \lesssim z \lesssim 1.6$ and to detect absorption/emission lines of each galaxies with high signal-to-noise ratios ($S/N \gtrsim 5$–10) for a reasonable amount of exposures (about one hours per field). Thus the SuMIRe survey offers an exciting opportunity to map the three-dimensional distributions of dark matter, galaxies and clusters over a wide range of redshifts extending out to $z \simeq 1.6$. We will combine the imaging and redshift data sets of the *same* sky region and from the *same* telescope in order to conduct the dark energy experiments and to test gravity on cosmological scales, by minimizing systematic errors inherent in each method. The unique data sets also enable us to study various additional science cases such as galaxy evolution.

The HSC wide-field, multi-color (*grizy*) survey covering about 2000 square degree area is now being planned to start from 2012 for 5 years and will enable us to measure weak lensing signals of distant galaxy images as a function of angular scales and redshifts as well as to find massive clusters out to $z \simeq 1.5$ based on the available photometric redshift information (its high-redshift sensitivity thanks to the presence of deep y-band data). By maximizing an overlap of the HSC survey region with the survey region of the Sunyaev-Zel'dovich experiment with the Atacama Cosmology Telescope (ACT), the robust cluster experiment becomes available by using the combined mass-proxy relations from all the available optical, lensing and SZ information. Another survey mode, the multi-color, multi-epoch "deep" survey with HSC covering a few tens of square degree field, is also planned, which enables us to find supernovae at high redshifts and then carry out the luminosity distance experiments if the spectroscopic follow-up campaign to obtain their redshifts is properly coordinated.

However, the most damaging systematic errors inherent in the imaging-based experiments arise from photometric redshift errors. The photometric redshift errors can be robustly calibrated by carrying out a spectroscopic redshift survey with PFS for the HSC survey region delivering spectroscopic redshifts for a few millions of galaxies. More promisingly the PFS redshift survey itself enables us to carry out the BAO experiment using galaxies over a redshift range of $0.6 \lesssim z \lesssim 1.6$, which can have a similar-level constraining power of dark energy with the HSC dark energy experiments and is complementary to the existing/ongoing BAO surveys such as the SDSS and BOSS surveys that cover the range $0 \lesssim z \lesssim 0.65$. The target galaxies for the PFS survey can be delivered from the sufficiently deep HSC data. The redshift distortions due to peculiar velocities of galaxies, if robustly measured, can be used to further improve the cosmological constraints as well as the ability to test gravity on cosmological scales. The expected constraints on dark energy parameters, neutrino masses and primordial non-Gaussianity parameter are summarized in Table 5.

1 Key Science Goals

1.1 HSC imaging survey

Let us start our discussion with the planned HSC survey which will give an ideal, pre-imaging survey to find target galaxies for the PFS redshift survey. We are currently planning to carry out three different surveys (wide, deep and ultra-deep) with HSC, and Table 1 give survey parameters of the planned HSC-wide and -deep surveys (although not finalized). The HSC wide survey can achieve new parameter space, deeper by more than one magnitude and greater in surveyed comoving volume by more than a factor 10 than the

Table 1: HSC imaging survey

	Area [sq. deg.]	Depth [AB, 5σ, $2''$]	Methods	redshifts
HSC-Wide	1500-2000	$g(26), r(25.9), i(25.8), z(25), y(24)$	WL , Cluster	$z \lesssim 1.5$
HSC-Deep	$\sim$30	$grizy$+NBs ($i \simeq 27.2$)	$\sim$ 500SNe	$0.4 \lesssim z \lesssim 1.2$

The magnitudes mentioned are derived assuming a point source for 5σ detection and $2''$ aperture.

Table 2: SuMIRe Dark Energy Experiments: Dominant systematic errors of each method and the SuMIRe methods of controlling those errors

Methods	Dominant systematic errors	SuMIRe approaches
Weak lensing	Photo-z errors	PFS data (spectroscopic calibration sample)
	Shape measurements	Subaru image-quality, methods & algorithms
	Small-scale clustering	A suite of high-resolution simulations
Clusters	Mass-observable relations	SZ-optical-lensing cross calibration
	Selection function	PFS spectroscopic calibration of BCGs
BAO	Galaxy biases	Lensing-galaxy cross-correlations
	Nonlinearities	A suite of simulations & refined analytical methods
Type-Ia supernovae	Photometric calibration	Calibration strategy, spectroscopic calib.

existing surveys thanks to the photon collecting power of the 8.2m Subaru Telescope. The HSC-wide survey is also deeper than the planned DES survey by about 1.5 magnitudes in i band. Furthermore, with the advent of the fully depleted CCD chips, the HSC survey can achieve a unique depth in red bands, thereby significantly improving signal-to-noise ratios in imaging red galaxies at higher redshifts.

By having the HSC-wide survey, we can carry out various cosmological experiments. In particular, the unique capabilities of the Subaru Telescope, its photon collecting power and superb image-quality, achieve high-precision measurements of weak lensing distortions of distant galaxy images due to cosmic hierarchical structures. This weak lensing is a powerful way of measuring the dark matter distribution as well as the angular diameter distance combination [43]. Furthermore, we will plan to maximize an overlap of the HSC survey region with the ACT SZ survey region [3]. The SZ effect is independent of redshift, therefore a very powerful way of finding massive clusters out to high redshifts. The HSC multi-band data can not only determine redshifts of SZ-found clusters out to high redshifts $z \simeq 1.5$ based on the photometric redshifts, especially by having the deep y-band data, but also enable us to make lensing-based mass calibration of the clusters in individual and statistical bases. Thus the HSC-ACT data sets can provide us with a unique catalog of massive clusters that extends out to $z \simeq 1.5$. We will use both the weak lensing observables and the cluster counting statistics in order to constrain cosmological parameters [42].

The primary science driver of the planed HSC-deep survey is to survey type-Ia supernovae (SNe). The depth and wide-field capabilities allows for obtaining light curves of over 500 supernovae. We will thus carry out the luminosity distance measurement with the SNe sample, however, the spectroscopic follow-up campaign needs to be properly coordinated, which is not yet finalized.

The dark energy experiments, weak lensing, cluster counting statistics, and SNe, are summarized in Table 2, and the dominant systematic errors inherent in each method are also given.

1.2 PFS Survey and Requirements

The PFS survey will bring a great synergy with the HSC survey. The deep, multi-color HSC data sets can deliver an ideal catalog to find target galaxies for the PFS redshift survey based on the same telescope. To maximize the synergy of HSC and PFS surveys we can choose, as the target galaxies, red galaxies (BCGs and early-type galaxies) in cluster regions and star-forming blue galaxies. By targeting emission-line [OII] (3726Å, 3729Å) for blue galaxies in high-redshift side, we can probe the three-dimensional galaxy distribution over a wide range of redshifts, $0.6 \lesssim z \lesssim 1.6$, which then becomes complementary to the ongoing BOSS survey with redshift range $0.4 \lesssim z \lesssim 0.65$ and 10000 square degree area (mostly in the northern hemisphere sky). Thus we can use the combined spectroscopic data sets from the BOSS and PFS surveys

Table 3: PFS Survey Parameters

Redshift	V_s $[h^{-3}\mathrm{Gpc}^3]$	N_g (per field)	$\bar{n}_g[h^3\mathrm{Mpc}^{-3}]$	b	$\bar{n}_g P_g@k = 0.1h\mathrm{Mpc}^{-1}$
$0.6 < z < 0.8$	0.8	212	3×10^{-4}	1.5	1.4
$0.8 < z < 1.0$	1.1	292	3×10^{-4}	1.5	1.2
$1.0 < z < 1.2$	1.4	495	4×10^{-4}	1.5	1.3
$1.2 < z < 1.4$	1.6	565	4×10^{-4}	1.5	1.2
$1.4 < z < 1.6$	1.7	600	4×10^{-4}	1.5	1.0

Note: The total number of target galaxies is 2164 per the SuMIRe PFS field-of-view. We assumed that the linear bias parameters of target galaxies $b = 1.5$ all the redshift slices according to some studies [8, 7, 40], but the actual values are still uncertain. If we can preferentially target early-type galaxies which tend to have greater biases such as $b \simeq 2.3$ for LRGs, it can relax requirements on the number density of target galaxies by up to 50%($\simeq 2.3/1.5$).

to calibrate dominant systematic errors in the weak lensing and cluster experiments; photometric redshift errors and cluster selection function.

More importantly the PFS data sets themselves allow us to carry out another dark energy experiment, the baryonic acoustic oscillation (BAO) experiment, from the measured three-dimensional distribution of over a million of galaxies. The BAO method is now recognized as the method "least affected" by systematic uncertainties among the dark energy experiments, as demonstrated in the actual measurements [12, 9]. By measuring the BAO length scale imprinted on the galaxy distribution in both the directions along and perpendicular to the line-of-sight direction for the HSC survey region of 2000 square degrees, we can achieve high-precision measurements of the angular diameter distances and the Hubble expansion rates over the redshift range $0.6 \lesssim z \lesssim 1.6$ with precisions of a few percent (see Figure 1). Although the most dangerous uncertainty in the BAO experiment arises from nonlinear, scale-dependent galaxy bias, the combined HSC and PFS surveys allow us to observationally disentangle the galaxy bias uncertainties by cross-correlating the galaxy distribution with the total matter (mostly dark matter) distribution reconstructed from the HSC weak lensing measurements. We can then use broad-band shapes of the galaxy power spectrum measured as a function of redshifts, which greatly improves the cosmological constraints and now opens up a window for constraining the growth of structure with the galaxy power spectrum [44, 41, 32, 33]. Furthermore, we may be able to use, if robustly measured, redshift distortions in the galaxy distribution caused by the peculiar velocities in order to further improve the cosmological constraints [46].

Thus the SuMIRe (HSC + PFS) survey enables us to carry out both the geometrical measurements (BAO + SNe) and the experiments probing the growth of structure (WL + Cluster + Galaxy Clustering). The combined experiments are very powerful and convincing in several aspects. First, the combined experiments not only provide the precise dark energy experiments, but also allow us to carry out a model-independent test of the metric gravity theory on cosmological length scales as follows. The different structure formation probes are sensitive to different combinations of the metric perturbations, gravitational potential and curvature perturbations, while the Einstein gravity predicts that the two perturbations are equal on all the relevant scales. Therefore, given the expansion history precisely constrained by the geometrical probes, we can now address if all the structure formation probes are consistent with the Einstein gravity predictions as a function of length scales and redshifts [14]. Second, by having the different methods, we can cross-check and self-calibrate various systematic uncertainties inherent in the methods in order to derive robust constraints on cosmological parameters. Finally, we can use the combined structure formation probes to explore constraints on a much broader range of variant models: neutrino masses, models of clustered dark energy and primordial non-Gaussianity [41, 32, 33, 17, 29, 34].

In summary the key science goals for the SuMIRe survey are

- Dark energy (WL, BAO, Galaxy Clustering, Cluster, SNe)
- Growth of structure (WL, Galaxy Clustering, Cluster)
- Neutrino mass (WL, Galaxy Clustering, Cluster)
- Primordial non-Gaussianity (WL, Galaxy Clustering, Cluster)

We now move on to requirements on the PFS specifications in order to achieve the key science goals above. The requirements come mainly from two factors: the number density of target galaxies and the redshift determination accuracy. As described above, the primary target galaxies are (1) brightest central

Table 4: Requirements on PFS Performance

Wavelength [nm]	Spectral Resolution	S/N	# of target galaxies per field	Angular size of fiber
∼600-1000	$R \sim 3000$	$\gtrsim$ 5-10/line for $i_{\rm AB} \lesssim 22.7$	~ 2200	$1\farcs2$ – $1\farcs4$ in diameter

Note: The quoted number of target galaxies per field assumes 100% success rate. If we have 80% or 90% success rates of selecting target galaxies, the number of target galaxies is increased to 2750 or 2444, respectively. Note that the BOSS survey is currently achieving about 90% success rate in selecting LRGs from the photometric data.

galaxies (BCGs) in HSC-ACT found cluster regions and early-type galaxies and (2) star-forming blue galaxies exhibiting [OII] emission lines. The statistical precision of the BAO scale measurement is determined by the shot noise and the sampling variance. To achieve the nearly sampling variance limited regime for a fixed survey area, we need to sample target galaxies with number densities satisfying $\bar{n}_g P_g \gtrsim 1$ at BAO scales ($k \simeq 0.1h{\rm Mpc}^{-1}$), where $\bar{n}_g$ is the mean comoving number density of galaxies and P_g is the galaxy power spectrum amplitude at the BAO scales. Assuming the WMAP 7-year cosmology, we can find that the required total number of galaxies is about 2×10^6 galaxies for a survey with 2000 square degrees assuming the redshift coverage $0.6 \lesssim z \lesssim 1.6$. Or this corresponds to about 2200 galaxies per the PFS field-of-view (about 1.8 square degrees) as given in Table 3.

Another important factor we should take into account is the accuracy of redshift determination; the BAO measurement requires redshifts of galaxies to be measured with a percent-level precision in $(1+z)$ (see Fig. 7 in [36]). Hence the absorption/emission line(s) of each galaxy needs to be detected with a sufficiently high signal-to-noise ratio (greater than $S/N \simeq$ 5-10). In particular, to cover high redshifts $1.2 \lesssim z \lesssim 1.6$, [OII] emission line (3726Å) needs to be detected in red bands beyond 8000 Å, where there are many OH sky lines.

Hence the requirements on the PFS specifications are summarized as

- Enable us to cover redshift range $0.6 \lesssim z \lesssim 1.6$ making the PFS BAO survey complementary to the ongoing BOSS survey that covers $0.4 \lesssim z \lesssim 0.65$
- Enable a multi-object spectroscopic observation of brightest central galaxies (BCGs) in the HSC-ACT found cluster regions, early-type galaxies and [OII] emission-line galaxies ([OII]: 3726Å) in order to maximize its synergy with the HSC survey
- Need to obtain about 2200 spectra per the PFS field-of-view in order to make the BAO experiment be in the sampling variance limited regime, which satisfies $\bar{n}_g P_g \simeq 1$ at BAO scales ($k \simeq 0.1h{\rm Mpc}^{-1}$)
- Absorption/emission line(s) of each galaxies needs to be detected with a high signal-to-noise ratio ($S/N \gtrsim$ 5–10) in order to have a percent-level determination of galaxy redshifts
- Need to discriminate [OII] emission line from OH sky emission lines in red bands (> 8000 Å)

As described below in detail (see § 1.4), we used the zCOSMOS redshift catalog of galaxies (*real data!*) in order to study what kinds of galaxies and how many galaxies are available. The zCOSMOS catalog contains the HST/ACS i-band selected galaxies $i_{\rm AB} \leq 22.5$ for the COSMOS survey area (1.7 square degrees), where the spectra of galaxies have been taken by the VLT telescope for about one hour exposures and with spectral resolution $R \simeq 600$ for wavelength range 5550–9650Å. We found that, up to $z \lesssim 1.2$, there are a sufficient number of galaxies satisfying the required number densities of galaxies in Table 3, if we include earl-type galaxies and blue galaxies with [OII] emission line being detected with signal-to-noise ratios greater than 5. However, galaxies at $z \gtrsim 1.2$ (the zCOSMOS covers up to $z = 1.4$) are fewer than required for the PFS BAO surveys. Hence several improvements on the PFS specifications are needed to meet the requirements above: (1) if we have a higher spectral resolution such as $R \simeq 3000$, we can have a factor 2 improvement in the signal-to-noise ratios compared to the zCOSMOS. Such a high resolution is also very powerful to discriminate [OII] emission line from OH sky emission lines in red bands beyond 8000Å. (2) We can use red-sensitive CCD chips covering up to 10000Å as used in the HSC camera (the zCOSMOS have been using the CCD chips that are not as high sensitive in red as the HSC CCDs. The zCOSMOS catalogs contains i-band selected galaxies with $i_{\rm AB} \lesssim 22.5$ and did not fully use the photometric redshift information from the available multi-color. In this sense the zCOSMOS catalog can be considered to rather give an lower limit on the available galaxies especially at high redshifts $z \gtrsim 1.2$, where galaxies

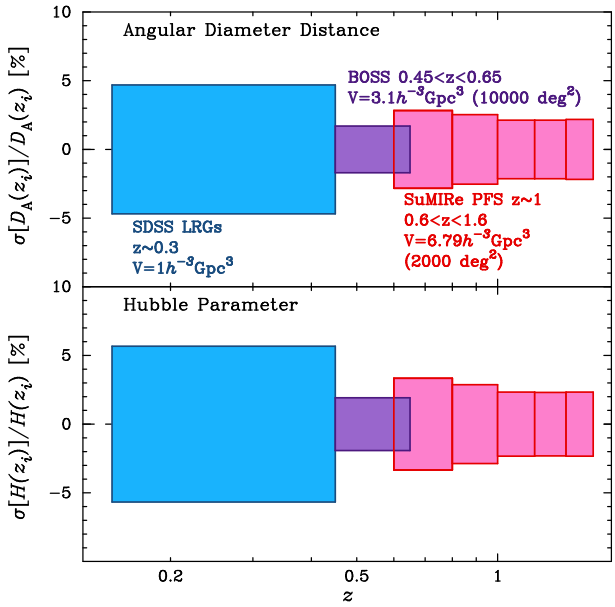

Figure 1: Fractional errors in measuring the angular diameter distance and the Hubble expansion rate for each redshift slices for the different BAO surveys, SDSS, BOSS and PFS. For the PFS survey we assumed survey parameters given in Table 3. Note that the expected accuracies of distance measurements are sensitive to the bias parameters or number densities of target galaxies we assumed.

tend to be brighter in redder bands than in i band. Therefore a more careful study for target galaxies for the PFS survey needs to be done assuming the deep, multi-color data sets available from the HSC-wide survey.

The requirements on the PFS performance are summarized in Table 4. We found that, if we can obtain redshifts for galaxies with $i_{AB} < 22.7$, the required number of targets per field seems available. A requirement on the angular size of each fiber simply comes from the fact that the median seeing size at the Subaru Telescope site is typically 0.6–0.7″ FWHMs. A fiber having a size larger than the FWHMs by a factor 2 would not have a significant contamination from sky.

Figure 1 shows the expected accuracies of measuring the angular diameter distances and the Hubble expansion rate for each redshift slices assuming the survey parameters in Table 3 for the PFS BAO survey. It can be seen that the PFS BAO survey can achieve a few percent accuracies of the distance measurements and is quite complementary to the SDSS and BOSS surveys, yielding a wider coverage of redshifts out to $z \simeq 1.6$. The dark energy contribution to the cosmic expansion becomes insignificant at $z \gtrsim 1$, if dark energy is equal or close to the cosmological constant, and therefore the PFS survey combined with the SDSS and BOSS can open up a window to test early dark energy models up to $z \simeq 1.6$.

Next let us estimate the expected performances of the PFS BAO survey and the SuMIRe survey, i.e. a joint experiment of the HSC imaging survey and the PFS redshift survey. Table 5 shows the parameter forecasts, where we assumed the WMAP 5-year cosmology as the fiducial model. For all the forecasts we assumed the Planck CMB prior on cosmological parameters (see [33] for the details). For the BOSS and PFS surveys we assumed that the surveys are used to carry out the pure geometrical test for constraining the dark energy equation of state parameters. That is, we did not include the broad-shape and amplitude information of galaxy power spectrum for the BAO surveys. The dark energy figure-of-merit quantity studied in the Report of Dark Energy Task Force, named as "DETF FoM" in Table 5, is defined as DETF FoM$\equiv [\sigma(w_0)\sigma(w_a)]^{-1}$ assuming that the dark energy equation of state is parametrized as

$$w(a) = w_0 + (1-a)w_a. \tag{1}$$

Table 5 clearly demonstrates that adding the PFS BAO survey in the BOSS survey can improve the FoM value by a factor 3 compared to the BOSS survey alone, reflecting that the BOSS and PFS surveys are indeed complementary.

The forecast for the SuMIRe survey shows the results for the combined HSC and PFS surveys (note the HSC imaging survey will be already done before the PFS survey starts). Here we assumed a joint experiment

Table 5: Parameter Forecasts

	BOSS	PFS(+BOSS)	SuMIRe (BOSS+PFS+HSC)
Redshift	$0.2 < z < 0.65$	$0.6 < z < 1.6$	$0 \lesssim z \lesssim 1.6$
Sky Coverage	10000 deg^2	2000 deg^2	2000 deg^2
$\sigma(w_0)$	0.083	0.046	0.028
DETF FoM	13	33	217
Growth: $\sigma(\gamma)$	-	-	0.032
$\sigma(\sum m_\nu)$ [eV]	-	-	0.06 eV
$\sigma(f_{\rm NL})$	-	-	$\sim$5

Note: The Planck CMB prior and SDSS LRGs constraints are assumed for all the surveys. The forecasts for BOSS and PFS are based on the assumed BAO experiments, and we did not include information in the overall shape and amplitudes of galaxy power spectrum. Therefore the dark energy constraints shown are conservative. The forecasts for SuMIRe (PFS+HSC+BOSS) are computed assuming the hypothetical joint experiments of weak lensing, cluster, BAO and galaxy clustering, where we included the overall shape and amplitude information of galaxy power spectrum assuming that galaxy bias uncertainties can be calibrated by comparing the galaxy and lensing-reconstructed matter distributions. However a more careful, realistic forecast needs to be studied (this is in progress).

of BAO, weak lensing and cluster counting statistics, and also included the broad-band shape and amplitude information of the PFS galaxy power spectrum to constrain cosmological parameters assuming that bias uncertainties of galaxies can be observationally disentangled via the cross-correlations of weak lensing, cluster distribution and galaxy distributions. The table shows that the SuMIRe survey is very powerful to obtain the precise dark energy constraints: it can improve the dark energy FoM value by a factor 6 over the PFS BAO survey. The joint experiment now allows us to test the growth of structure formation. To estimate the ability of SuMIRe for constraining the growth of structure, we used the approach proposed in [2]: the linear growth rate of density perturbation is parametrized as

$$G(a) \propto \exp\left(\int^a d\ln a' \left[\Omega_{\rm m}^{\gamma}(a') - 1\right]\right) \tag{2}$$

where $G(a) \equiv \delta(a)/a$ is the linear growth of density perturbations normalized to Einstein de-Sitter case, γ is a parameter (see below), and $\Omega_{\rm m}(a)$ is the density parameter of total matter relative to the critical density at redshift $z\,[= 1/a - 1]$. The value $\gamma = 0.55$ is shown to closely approximate the exact solution within general relativity for a wide variety of dark energy equation of state models [27]. That is, measuring a departure of γ from the fiducial value ($\gamma = 0.55$ for ΛCDM) provides a test of general relativity on cosmological scales. Table 5 shows the expected accuracy of constraining the γ parameter, $\sigma(\gamma)$, where the error on γ includes marginalization over other cosmological parameters including the dark energy equation of state parameters w_0 and w_a. The SuMIRe survey can achieve a few percent accuracies of constraining the γ parameter.

In Table 5 we also show the ability of SuMIRe survey for constraining neutrino masses as well as the primordial non-Gaussianity parameter $f_{\rm NL}$. The sum of neutrino masses can be constrained with a precision of $\sigma(\sum m_\nu) \simeq 0.06$ eV, meaning that the neutrino masses can be detected at better than a 2σ level if the neutrinos obey the inverted mass hierarchy that predicts the sum of neutrino masses to be $\sum m_\nu \gtrsim 0.11$ eV. Furthermore, the primordial non-Gaussianity can be probed by using the unique catalog of massive clusters available from the SuMIRe survey, because the primordial non-Gaussianity is shown to change the abundance of massive clusters and also induce a scale-dependent halo bias. The effect is more significant for more massive halos. Table 5 shows that the SuMIRe can achieve the accuracy of $\sigma(f_{\rm NL}) \simeq 5$ [29] for the constraint on the primordial non-Gaussianity parameter $f_{\rm NL}$. This precision is similar to that expected from the Planck CMB experiment, however, the SuMIRe can constrain the primordial non-Gaussianities on different length scales and at different redshifts.

1.3 Effective survey depth

We estimate the exposure times required to reach a given sensitivity in order to assess the feasibility of carrying out a wide field survey (>1000 square degrees) in a reasonable amount of observing time. In

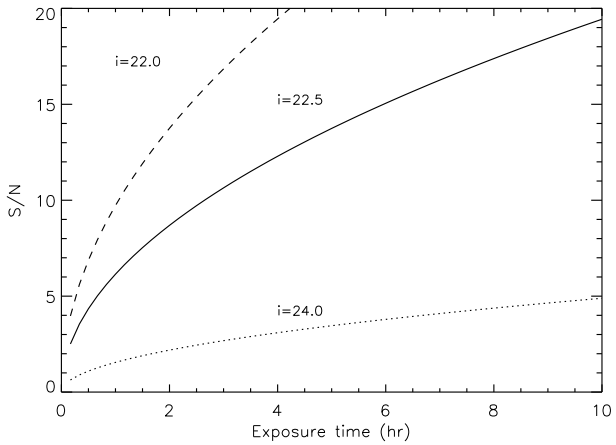

Figure 2: Signal-to-noise in the continuum as a function of exposure time in hours for a hypothetical SuMIRe setup. Curves show expected results for three different limiting magnitudes.

Table 6: Hypothetical values for a Subaru/SuMIRe setup

Parameter	Value
Spectral resolution ($\Delta\lambda$)	4 Å at 8000 Å (R=2000)
Spectral sampling	1 Å pix^{-1}
Fiber size (diameter)	$1.5''$
Pixel scale	$0.3''$ pix^{-1}
CCD QE	85%
Filter transmission	90%
Total telescope+instrument throughput	10%

Figure 1.3, we show the expected signal-to-noise (S/N) ratio for a given limiting magnitude as a function of total on-source exposure time for a flat continuum. We see that an hour is sufficient to reach a S/N of 5 in the continuum per resolution element for an object with $i_{AB} = 22.5$ and $S/N = 10$ for $i_{AB} = 22.0$. These limits are based on rough estimates of telescope+instrument performance as given in Table 6. We note that the performance is likely to be better with a higher total throughput and smaller fibers with diameters of $1-1.3''$. We note that fiber-to-fiber variations in the sky measurements and a time-variable sky can degrade performance. Although, an implementation of nod and shuffle will allow for sky background subtraction through the equivalent fiber and detection on the same CCD pixels as the source spectrum.

1.4 Target galaxies

Our survey design is chosen to provide a galaxy sample of sufficient size that can meet the science requirements for the BAO and weak lensing studies as outlined above. An evaluation of the target density is therefore warranted. To do so, we estimate the observed surface density of galaxies with $0.8 < z < 1.4$ using the 20k spectroscopic redshift catalog of zCOSMOS, kindly provided by the team (P.I. Simon Lilly-ETH Zurich). The zCOSMOS 'bright' sample is a flux-limited ($i_{AB} < 22.5$) spectroscopic survey of 20,000 galaxies randomly selected over 1.7 sq. degrees in the COSMOS field using VIMOS on the VLT. One hour exposures are taken to acquire spectra of sufficient signal-to-noise to measure redshifts out to $z \sim 1.2$. The instrumental setup is chosen with a spectral wavelength coverage of 5500-9700 Å, a spectral resolution ~ 12 (R=600), and a velocity accuracy of ~ 100 km s^{-1} as determined by repeat observations. This survey enables us to determine the surface density of potential Subaru PFS targets as a function of galaxy color and stellar mass. Survey parameters (e.g., limiting magnitude, wavelength coverage) are close to those planned for the Subaru PFS. Although, we highlight that the PFS is likely to have an improved sensitivity in the red as compared to the VIMOS gratings and CCDs, and higher resolution ($R \sim 3000$). Two samples of galaxies will be specifically isolated: (1) luminous (i.e., massive) red galaxies, and (2) emission-line (i.e., star-forming) galaxies. Even though the redshift range of a future PFS survey will extend out to $z \sim 1.5$, the zCOSMOS survey can provide detailed information on the dominant source populations in such a Sub-

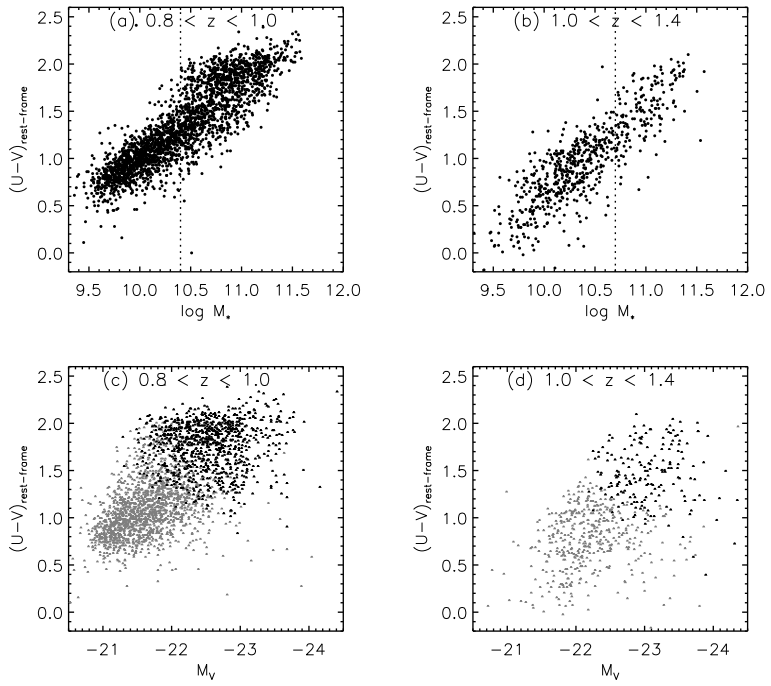

Figure 3: Rest-frame color of zCOSMOS galaxies as a function on their stellar mass (panels *a*-*b*) and absolute magnitude (panels *c*-*d*). Two redshift intervals are shown. The vertical lines in the top panels show the limiting mass for which the zCOSMOS sample is fairly complete. Massive galaxies (log $M_\star > 10.7$) are marked in black in the lower panels.

aru survey and provide an assessment of the redshift success rate (See Fig. 2 and 3 of [26]) for faint targets at high redshift.

1.4.1 Massive galaxies at $0.8 < z < 1.4$

We chose to use similar galaxy tracers (i.e., luminous red galaxies) of BAO as done with the SDSS [12]. Here, we will address these galaxies by their high stellar mass that is essentially the luminous population. This enables us to present a single sample of galaxies to be used for the determination of cosmological parameters and the studies of galaxy evolution to be discussed below. In Figure 1.4.1, we plot the distribution of rest-frame color of zCOSMOS galaxies as a function of their stellar mass and rest-frame absolute magnitude. Two redshift intervals are shown that are most relevant for a SuMIRe PFS survey. First of all, it is apparent that the number of massive galaxies (log M > 11) is small in a field of 1.7 square degrees. This is most apparent at high redshift ($1.0 < z < 1.4$) with less than 100 galaxies with these masses. In Table 2, we provide some statistics regarding the zCOSMOS sample. To be clear, these are the number of galaxies with successful redshift measurements. From these numbers, we estimate the number of potential SuMIRe/PFS targets per pointing (rightmost column). The estimate takes into consideration the 70% sampling rate of zCOSMOS but not the redshift success rate that is roughly 90% for blue galaxies and 80% for red galaxies at $z \sim 1$ but can reach down to 60% at $z > 1.2$. We see that there are potentially ∼1413 galaxies having $0.8 < z < 1.4$ per SuMIRe/PFS pointing but most of these have redshifts between 0.8–1.0. An improvement in the number of targets for the PFS may require reaching fainter depths in a flux-limited i-band survey and a z-band selected sample.

1.4.2 Emission-line galaxies at $0.8 < z < 1.4$

Star-forming galaxies are also a target for BAO studies due to their prevalence at $z \sim 1$. The emission line doublet [OII]$\lambda 3726, 3729$ is a prominent spectral feature that greatly facilitates redshift determination especially at the red end of the spectrum that is usually plagued by strong night-sky emission lines.

Here, we assess the magnitude of such a star-forming population based on the zCOSMOS 20k spectroscopic catalog as done for the massive/luminous galaxies. Most commonly used spectral features (i.e., emission and absorption lines) have been measured in an automated procedure (see [23] for details) for each zCOSMOS galaxy. In Figure 1.4.2*a*, we plot the rest-frame color versus absolute magnitude for zCOSMOS

Table 7: Massive zCOSMOS galaxies with $i_{AB} < 22.5$

Redshift range	Mass log $M_\star$	Red galaxies (U–V>1.6)	Blue galaxies (U–V<1.6)	# per SuMIRe pointing[1]
$0.6 < z < 0.8$	> 10.4	1135	548	2545
$0.8 < z < 1.0$	10.4–10.7	139	331	710
$0.8 < z < 1.0$	> 10.7	619	154	1169
$1.0 < z < 1.4$	> 10.7	62	99	244
Total ($0.8 < z < 1.4$):	> 10.7	681	253	1413

(1) These estimates include the 70% sampling rate of zCOSMOS and the difference between the survey area of zCOSMOS and a single SuMIRe/PFS pointing (1.8/1.7).

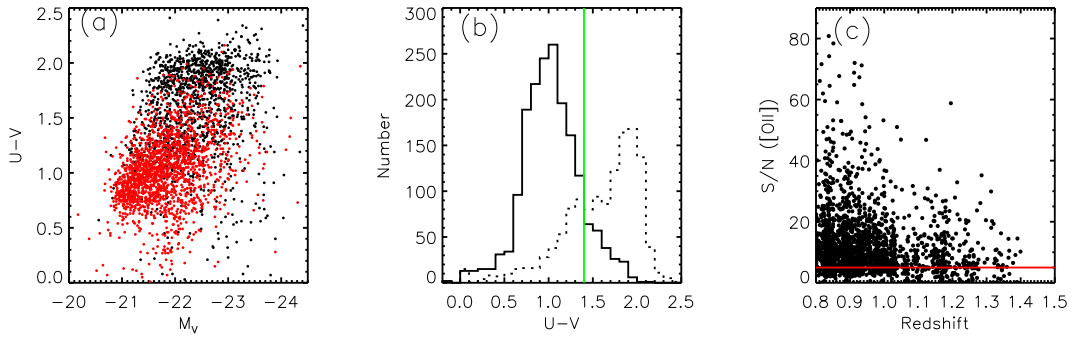

Figure 4: zCOSMOS galaxies with [OII]λ3726 detections. Rest-frame color vs. absolute magnitude: (panel a) galaxies with secure [OII] detections ($S/N > 5$) are marked in red while those with $S/N < 5$, including non-detections, are shown in black. In panel *b*, we show the histogram of galaxies with $S/N > 5$ (solid line) and all others (dotted line). A vertical green line marks the section of blue-galaxies ($U - V < 1.4$) for a future SuMIRe surveys. The S/N for all galaxies with $U - V < 1.4$ is shown in panel *c*.

galaxies with $0.8 < z < 1.4$. We highlight those objects with a detection of [OII] with significance (essentially signal-to-noise ratio) greater than 5. This significance represents a secure detection that will yield an accurate redshift in all such cases. In Figure 1.4.2, we show some example spectra from zCOSMOS with their [OII] detection significance given in each panel.

It is important to consider the selection of such a population of star-forming galaxies for a wide field survey with SuMIRe/PFS. In Figure 1.4.2*a*, *b*, it is evident that the strength of [OII] can vary even for blue and red galaxies. For a cut of $U - V < 1.4$, we find that 81% have [OII] detections with a $S/N > 5$ (see panel b). In Fig. 1.4.2*c*, we plot the [OII] emission line significance versus redshift for only galaxies with $U - V < 1.4$. Is it clear that a significant number of galaxies have $S/N < 5$. We note that redshifts are likely to be robust for galaxies with $S/N > 5$ in a SuMIRe/PFS survey although their detection may be compromised in areas of significant night-sky emission. In Table 3, we list the number of such star-forming galaxies in zCOSMOS and that expected in a single SuMIRe/PFS pointing that are not included in the mass selected sample discussed above. We estimate that there will be ∼2337 star-forming galaxies with $U - V < 1.4$ and at $0.8 < z < 1.4$ per SuMIRe pointing. We point out that a substantially smaller number (517) are at $z > 1$. As mentioned above, the target density is likely to be higher given the technical specifications of SuMIRe/PFS and implementing a survey strategy aimed at the high-z population.

Table 8: Emission-line galaxies in zCOSMOS with $i_{AB} < 22.5$ and $U - V < 1.4$

Redshift range	S/N>3	S/N>5	S/N>10	# ($S/N > 5$) per SuMIRe pointing[1]
$0.8 < z < 1.0$	1361	1203	748	1820
$1.0 < z < 1.4$	406	342	178	517
Totals:	1767	1545	926	2337

(1) These estimates include the 70% sampling rate of zCOSMOS and the difference between the survey area of zCOSMOS and a single SuMIRe pointing (1.8/1.7).

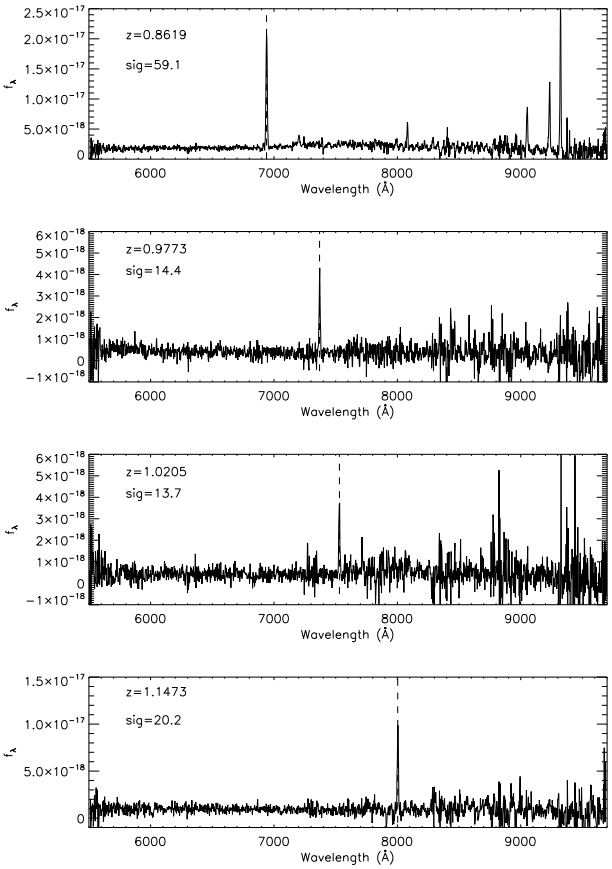

Figure 5: Example spectra of zCOSMOS galaxies with clear [OII] detections ($S/N > 10$).

2 Additional Science Cases

2.1 SuMIRe/PFS wide-area survey: Massive galaxy formation at $z \sim 1$

Remarkable advances in our understanding of galaxy evolution have been made from large spectroscopic surveys from the SDSS (e.g., [20]) at low redshift to $z \sim 1$ with zCOSMOS [26], VVDS [24] and DEEP2 [10] to just name a few. A picture is emerging where the mass buildup is dependent on environment with star formation being truncated not only by such environmental factors (e.g., [48, 4]) but quenched by a mechanism that is not yet understood [30]. Likely candidates include feedback from supernova and Active Galactic Nuclei possibly triggered in major mergers of galaxies (e.g., [15]).

While current surveys are now providing large sample of galaxies up to redshifts of 1, they do not cover a sufficient volume, as comparable to SDSS at $z < 0.3$, to probe the most massive structures at $z \sim 1$. For example, only a handful of galaxy clusters with $M_{halo} > 10^{14} M_{\odot}$ are present within the survey volume of COSMOS field [22]. As well, the numbers of massive galaxies ($M > 10^{11} M_{\odot}$) are not of sufficient size to accurately tie down the high end of the mass function [6, 18] when split into those that are still actively forming stars or those of a more quiescent nature. With AGN more prevalent in the massive galaxies (e.g., [37]), a full understanding of the relation between galaxies and their supermassive black holes requires samples comparable to SDSS but at $z \sim 1$, an epoch of maximal growth.

A wide-field spectrograph mounted on an 8-m class telescope (i.e., Subaru) is unique in its capability to provide spectroscopic redshifts to limiting magnitudes comparable to current wide areas surveys such as zCOSMOS but over an area 600X larger. A wavelength range $\sim 5000 - 10000$ Å is ideal to acquire spectroscopic redshift for galaxies up to $z \sim 1.4$. Moderate-resolution spectra ($R \sim 3000$) will provide stellar velocity dispersions with an instrumental velocity resolution of ~ 50 km s^{-1}, star formation rates (based on [OII] strengths), stellar ages (e.g., Dn4000, HδA), metallicities, and diagnostics for identifying AGN activity [21]. With ~ 3000 apertures/fibers per configuration, it is possible to complete a zCOSMOS-like program in under a week whereas ESO has taken 5 years. The scientific drivers for galaxy evolution studies with SuMIRe/PFS include the following:

- Evolution of the mass function of galaxies up to $z \sim 1.4$
- Clustering of massive galaxies at $z \sim 1$
- Optical spectroscopic properties of massive galaxies: Stellar populations and star formation rates
- Role of AGNs in massive galaxy formation

2.2 Quasars out to $z \sim 7$

Wide-area optical surveys, such as the SDSS (e.g., [35]) , have generated samples of over 100,000 quasars to investigate the growth of supermassive black holes up to $z \sim 6$ (e.g., [13]). Given the shallow depth of the SDSS survey, the selection restricts the samples to extremely massive black holes ($M_{BH} \sim 10^9 M_\odot$) especially at high redshift. Therefore, we have limited knowledge of the magnitude of the bulk of the quasar population since the co-moving space density is steeply rising toward lower luminosities [31] and masses [49]. Such uncertainty has not yet settled the issues at to whether quasars or stars are responsible for reionization at $z \sim 6$ that has led to much debate (e.g., Glikman et al. 2010; Oesch et al. 2010). Furthermore, the existence of such massive black holes at $z \sim 6$ may pose a challenge to our understanding of structure formation when the universe was less than one billion years old. Their rapid buildup has been attributed to processes such as super-Eddington accretion (e.g., [50]) or multiple episodes of major mergers of galaxies (e.g, [25]). Although, such analysis are based on a single object thus an adequate assessment of black hole growth at these early epochs requires knowledge their number distribution over a broader range in mass.

While current surveys are pushing to greater depths (e.g., [52, 51]), they lack the sky area to significantly improve upon those at high redshift. A wide-deep strategy such as planned for Subaru with Hyper-suprim Cam will probe the quasar population to fainter luminosities thus enabling us to accurately determine the preponderance of typical black holes (masses around $10^{7-8} M_\odot$) at $z > 6$.

Based on quasar number counts from the COMBO-17 [52] survey, we expect 450 quasars at $z > 1.2$ ($R_{mag} < 23.5$) per SuMIRe pointing (1.8 square degree). With an HSC survey covering 10^3 sq. degree, we expect to detect over 200,000 quasars (2× that provided by SDSS). Currently, there are 40 spectroscopically identified quasars at $z \sim 6$. With a wide-deep Subaru/HSC survey, we estimate that between $\sim 30 - 360$ quasars will be detected at $z \sim 6$. The order-of-magnitude uncertainty reflects our current lack of knowledge of the faint-end slope of the luminosity function.

3 Another SuMIRe/PFS option: BAO at $z \sim 3$ with Lyman break galaxies

A deep survey with SuMIRe/PFS offers great potential to utilize the wide area coverage and multiplexing to target the high redshift ($z \sim 3$) galaxy population to measure baryonic acoustic oscillations. A 100 sq. degree survey reaching depths of $i \sim 25$ can potentially detect 100,000 Lyman break galaxies selected by their optical colors (u-band and g-band dropouts; See [38]). The technical requirements for such a survey require the use of a blue-sensitive spectrograph (∼3500 - 6700 Ang.). Such a strategy has been employed with various surveys ([38, 5]) although typically having area coverage of less than one sq. degree. As well, the zCOSMOS survey has acquired 10k spectra of high redshift galaxies at $z > 1.5$ mainly selected as sBzK ([11]) or BX/BM ([39]) galaxies. Based on preliminary results from zCOSMOS Deep, it is clear that the redshift success rate drastically improves in a redshift regime ($z > 2$) where Lyα falls within the observed window. A benefit of working at blue wavelengths is the lack of interference from night sky emission features that typically plague the longer wavelengths. In addition to a BAO study, additional science investigations include (a) determining the luminosity function of Lyman break galaxies, (b) clustering at $2 < z < 4$, (3) ISM kinematics/galactic outflows, (4) stellar populations and star formation rates, and (5) presence of AGN.

References

[1] A. Albrecht, et al., "Report of the Dark Energy Task Force", astro-ph/0609591

[2] A. Albrecht, et al., "Findings of the Joint Dark Energy Mission Figure of Merit Science Working Group", arXiv:0901.0721

[3] Atacama Cosmology Telscope Project, http://www.physics.princeton.edu/act/

[4] I. Baldry, et al., "*Galaxy bimodality versus stellar mass and environment*, MNRAS, **373**, 469 (2006)

[5] R. Bielby et al., "*The VLT LBG Redshift Survey I: Clustering and Dynamics of 1000 Galaxies at* $z \sim 3$", arXiv:1005.3028

[6] M. Bolzonella, K. Kovac, L. Pozzetti et al., "*Tracking the impact of environment on the Galaxy Stellar Mass Function up to z 1 in the 10k zCOSMOS sample*", in press, arXiv:0907.0013 (2010)

[7] C. Blake, et al., "*The WiggleZ Dark Energy Survey: the selection function and z = 0.6 galaxy power spectrum*", arXiv:1003.5721, MNRAS in press

[8] A. Coil, et al., "*The DEEP2 Galaxy Redshift Survey: Color and Luminosity Dependence of Galaxy Clustering at z 1*", Astrophys. J. **672**, 153 (2008)

[9] S. Cole, et al., "*The 2dF Galaxy Redshift Survey: power-spectrum analysis of the final data set and cosmological implications*", Mon Not. Roy. Astron. Soc. **362**, 505 (2005)

[10] M. Cooper et al., "*The DEEP2 Galaxy Redshift Survey: the relationship between galaxy properties and environment at z 1*", **370**, 198 (2006)

[11] E. Daddi et al., "*A New Photometric Technique for the Joint Selection of Star-forming and Passive Galaxies at* $1.4 < z < 2.5$", Astrophy. J., **617**, 746

[12] D. Eisenstein, et al., "*Detection of the Baryon Acoustic Peak in the Large-Scale Correlation Function of SDSS Luminous Red Galaxies*", Astrophys. J. **633**, 560 (2005)

[13] X. Fan et al., "A Survey of $z > 5.8$ Quasars in the Sloan Digital Sky Survey. I. Discovery of Three New Quasars and the Spatial Density of Luminous Quasars at $z \sim 6$", Astron. J., **122**, 2833

[14] J. Guzik, B. Jain, M. Takada, "*Tests of Gravity from Imaging and Spectroscopic Surveys*", Phys. Rev. D **81**, 023503 (2010)

[15] P. Hopkins, T. Cox, D. Keres, L. Hernquist, "*A Cosmological Framework for the Co-evolution of Quasars, Supermassive Black Holes, and Elliptical Galaxies. II. Formation of Red Ellipticals*", Astrophy. J. **175**, 390 (2008)

[16] D. Huterer, M. Takada, G. Bernstein, B. Jain, "*Systematic Errors in Future Weak Lensing Surveys: Requirements and Prospects for Self-Calibration*", Mon. Not. Roy. Astron. Soc. **366**, 101 (2006)

[17] K. Ichiki, M. Takada, T. Takahashi, "*Constraints on Neutrino Masses from Weak Lensing*", Phys. Rev. D **79**, 023520 (2009)

[18] O. Ilbert et al., "*Galaxy Stellar Mass Assembly Between* $0.2 < z < 2$ *from the S-COSMOS Survey*", Astrophy. J**709**, 644 (2010)

[19] D. Jeong, E. Komatsu, "*Primordial Non-Gaussianity, Scale-dependent Bias, and the Bispectrum of Galaxies*", Astrophys. J. **703**, 1230 (2009)

[20] G. Kauffmann, T. Heckman, S. White et al. "*Stellar masses and star formation histories for* 10^5 *galaxies from the Sloan Digital Sky Survey*", MNRAS, **341**, 33 (2003)

[21] L. Kewley, B. Groves, G. Kauffmann, T. Heckman, "*The host galaxies and classification of active galactic nuclei*", Astrophys. J. **372**, 961 (2006)

[22] C. Knobel, S. Lilly, A. Iovino et al., "*An Optical Group Catalog to z = 1 from the zCOSMOS 10 k Sample*", Astrophys. J. **697**, 1842 (2009)

[23] F. Lamareille, J. Brinchmann, T. Contini et al.,"*Physical properties of galaxies and their evolution in the VIMOS VLT Deep Survey. I. The evolution of the mass-metallicity relation up to* $z \sim 0.9$", A&A, **495**, 53 (2009)

[24] O. Le Fevre et al. "*The VIMOS VLT deep survey. First epoch VVDS-deep survey: 11 564 spectra with 17.5 IAB 24, and the redshift distribution over* $0 < z < 5$", A&A, **439**, 845 (2005)

[25] Y. Li et al. "*Formation of $z \sim 6$ Quasars from Hierarchical Galaxy Mergers*", Astrophy. J., **665**, 187 (2007)

[26] S. Lilly et al.,"The zCOSMOS 10k-Bright Spectroscopic Sample", Astrophys. JS **184**, 218 (2010)

[27] E. V. Linder, "Cosmic Growth History and Expansion History", Phys. Rev. D **72**, 043529 (2005)

[28] T. Matsubara, "*Nonlinear perturbation theory with halo bias and redshift-space distortions via the Lagrangian picture*", Phys. Rev. D **78**, 083519 (2009)

[29] M. Oguri, "*Self-Calibrated Cluster Counts as a Probe of Primordial Non-Gaussianity*", Phys. Rev. Lett. **102**, 211301 (2010)

[30] Y. Peng, S. Lilly, K. Kovac et al., "*Mass and environment as drivers of galaxy evolution in SDSS and zCOSMOS and the origin of the Schechter function*", in press, arXiv:1003.4747 (2010)

[31] G. Richards, M. Strauss, X. Fan et al., "*The Sloan Digital Sky Survey Quasar Survey: Quasar Luminosity Function from Data Release 3*", Astron. J., **131**, 2766 (2006)

[32] S. Saito, M. Takada, A. Taruya, "*Impact of massive neutrinos on nonlinear matter power spectrum*", Phys. Rev. Lett. **100**, 191301 (2008)

[33] S. Saito, M. Takada, A. Taruya, "*Nonlinear power spectrum in the presence of massive neutrinos: perturbation theory approach, galaxy bias and parameter forecasts*", Phys. Rev. D **80**, 083528 (2008)

[34] S. Saito, M. Takada, A. Taruya, "*Constraining neutrino masses with SDSS LRG Power Spectrum*", in preparation

[35] D. Schneider, G. Richards et al. "*The Sloan Digital Sky Survey Quasar Catalog. V. Seventh Data Release*", Astron. J., **139**, 2360

[36] H.-J. Seo, D. Eisenstein, Astrophys. J. **598**, 720 (2003)

[37] J.D. Silverman et al., "*Ongoing and Co-Evolving Star Formation in zCOSMOS Galaxies Hosting Active Galactic Nuclei*", Astrophys. J. **696**, 396 (2009)

[38] C. Steidel et al., "*Lyman Break Galaxies at Redshift z 3: Survey Description and Full Data Set*", Astrophy.J., **592**, 728 (2003)

[39] C. Steidel et al., "*A Survey of Star-forming Galaxies in the* $1.4 < z < 2.5$ *Redshift Desert: Overview*", Astrophy.J., **592**, 728 (2004)

[40] M. Sumiyoshi, et al., "*Photometric H alpha and [O II] Luminosity Function of SDF and SXDF Galaxies: Implications for Future Baryon Oscillation Surveys*", arXiv:0902.2604 (2009)

[41] M. Takada, "*Can a Galasy Redshift Survey Measure Dark Energy Clustering?*", Phys. Rev. D **74**, 043505 (2006)

[42] M. Takada, S. Bridle, "*Probing dark energy with cluster counts and cosmic shear power spectra: including the full covariance*" New J. of Phys. **9**, 446 (2007)

[43] M. Takada, B. Jain, "*Cosmological parameters from lensing power spectrum and bispectrum tomography*", Mon. Not. Roy. Astron. Soc. **348**, 897 (2004)

[44] M. Takada, E. Komatsu, T. Futamase, "*Cosmology with High-redshift Galaxy Survey: Neutrino Mass and Inflation*", Phys. Rev. D **73**, 083520 (2006)

[45] R. Takahashi, N. Yoshida, M. Takada, et al., "*Simulations of Baryon Acoustic Oscillations II: Covariance matrix of the matter power spectrum*", Astrophys. J. **700**, 479 (2009)

[46] J. Tang, I. Kayo, M. Takada, "*Velocity Power Spectrum Reconstruction from A Galaxy Redshift Survey*", in preparation

[47] A. Taruya, T. Nishimichi, S. Saito, T. Hiramatsu, "*Nonlinear evolution of baryon acoustic oscillations from improved perturbation theory in real and redshift spaces*", Phys. Rev. D **80**, 123503 (2009)

[48] D. Thomas, C. Maraston, R. Bender, C. Mendes de Oliveira, "*The Epochs of Early-Type Galaxy Formation as a Function of Environment*", Astrophys. J, **621**, 673 (2005)

[49] M. Vestergaard, X. Fan et al., "*Mass Functions of the Active Black Holes in Distant Quasars from the Sloan Digital Sky Survey Data Release 3*", Astrophy. J, **674**, 1 (2009)

[50] M. Volonteri, M. Rees, "*Rapid Growth of High-Redshift Black Holes*", Astrophys. J., **633**, 624 (2005)

[51] C. Willott et al., "*The Canada-France High-z Quasar Survey: Nine New Quasars and the Luminosity Function at Redshift 6*", Astron, J., **139**, 906

[52] C. Wolf et al., "*The evolution of faint AGN between z = 1 and z = 5 from the COMBO-17 survey*", A&A, **408**, 499 (2003)